Available online at http://scik.org

J. Math. Comput. Sci. 11 (2021), No. 3, 3037-3051

https://doi.org/10.28919/jmcs/5613

ISSN: 1927-5307

FACTUAL FOREGROUND SEGREGATION AND GRADIENT BASED BIAS CORRECTION IN BRAIN MR IMAGES

A. FARZANA[†,*], M. MOHAMED SATHIK, S. SHAJUN NISHA

PG & Research Department of Computer Science, Sadakathullah Appa College, Tirunelveli, India

Affiliation of Manonmaniam Sundaranar University, Abishekapatti, Tirunelveli 627 012, Tamil Nadu, India

Abstract: The bias field is an inadmissible image glitch that evolved during the procedure of image acquisition. N3 (Non parametric Non uniform intensity Normalization) is one of the prominent and publicly available bias correction algorithms. N3 algorithm's efficiency is limited by the imprecise foreground segregation. To handle this dilemma this paper is proposing a technique by comprising kernel construction and gradient based bias correction, which efficiently extracts the foreground from the bias corrupted image and erodes the present bias. The dataset used here are collected from BrainWeb website. The performance indicators Coefficient of Variation for white, grey matter and Coefficient of Joint Variation are used in disclosing the conclusion in quantitative aspect.

Keywords: bias field; brain MRI; intensity non uniformity; N3.

2010 AMS Subject Classification: 68U10.

1. INTRODUCTION

There are several medical imaging modalities are presently used such as Magnetic Resonance Imaging (MRI), Ultrasound, Computed Tomography (CT), Angiography, x-ray, Positron

[*]Corresponding author

E-mail address: farzanajohn9086@gmail.com

[†]Reg.No:18211192162005, Research Scholar PhD

Received February 27, 2021

Emission Tomography (PET), etc. The prime purposes of medical images are scientifically examine the human anatomy, investigate the severances of diseases, and assist the physician in treatment planning. MRI images are broadly preferred as a result of its non ionizing character and precise illustration for soft tissues such as muscles, ligaments, fat, etc. The bias is an image flaw. Bias field is also known as shading, Intensity In Homogeneity (IIH) and Intensity Non Uniformity (INU). A shading effect is developed over original image and image intensities are overlapped. The underlying driver of predisposition can be characterized into two categories scanner and anatomy related shortcomings. Scanner related problems include RF coil non uniformity, static magnetic field In Homogeneity and eddy currents. The anatomy related shortcomings encompass patient position, shape and orientation of anatomy during the scanning procedure [1-6]. Expulsion of bias is a mandatory preprocessing to be carried over while incorporating computer assistance diagnosing. Prospective techniques used to eliminate bias constructed by scanner. Retrospective techniques used to correct bias developed by patient. Prospective methods incorporate shimming techniques, phantom based calibration, arrangement of Radio Frequency coils and building a new mathematical model to expel the bias construction [7, 8, 9, 10]. Retrospective techniques incorporates filtering, segmentation, histogram and surface based fitting methods to discard the bias constructed in medical images [11, 12]. Several prospective and retrospective techniques are recommended till date. An automatic Fuzzy C Means clustering technique fusing regional and global pixel intensities is recommended to correct bias present in liver MR Images [13]. Novel region based level set method is recommended to simultaneously correct the Intensity In Homogeneity and segment the images. But this proposed model incorporates limitations because of inappropriate region of interest extraction from image [14]. Coherent Local Intensity Clustering Technique is proposed for Intensity In Homogeneity correction depending upon local pixel intensities in the regions of brain MR Images. When images are deteriorated by severe Intensity In Homogeneity this technique fails to classify the edge pixels and performance of this algorithm is limited with respect to noise and bias spectrum [15]. Modified Possiblistic Fuzzy C Means algorithm is recommended for bias correction [16]. This technique incorporates local and global pixel

intensities to expel the bias. But this technique mistakenly removes the lower force data presents in the first picture. Modified Intensity Clustering models [17] is recommended for bias correction, but robustness of this model depends upon the initialization of cluster center. In paper [18] the author proposed bias correction strategy based upon level set method. This method yield misclassification of image intensities when region and background tissues share same intensity. Non parametric Non uniform intensity Normalization (N3) is recommended for bias correction [19]. This is one of the efficient, mostly used and publicly available bias correction algorithms.

This paper is based over the outcome of authors previous work [21] where four contemporary IIH correction algorithms LEMS [22], MICO [23] BCFCM [24], and N3 are scrutinized at various levels over large amount of bench mark dataset and concluded that N3 outperforms the other algorithms in bias correction. N3 algorithm modeled bias as a smooth and gradually varying multiplicative field. This algorithm corrects the bias at several stages. It initiated with extracting foreground from the bias corrupted brain MR images. The extracted foreground is remodeled into working resolution. Sub sampling is performed to cut down the enforcement of aliasing and the derivative outcome is log transformed to peruse on lower intensity pixels. For sharpening values Full Width Half Maximum (FWHM) and probability density function are calculated. Bias field is approximated using Deconvolution filter and Gaussian blurring kernel. The predicted bias is smoothened using the B – spline. Once the convergence criterion met, the algorithm stops the iteration and performs inverse transform of image interpolation. N4 algorithm is recommended for bias correction [20] which is the improvement of N3 algorithm. It substitutes B –spline by incorporating modified optimization technique. Both of these methods start from extracting foreground. And all other bias correction operations implemented over the extracted foreground. No prior operations are carried out before foreground extraction. The problem comes here is, foreground cannot be extracted precisely from the bias corrupted image. Efficiency of this algorithm might be degraded while extracting inaccurate foreground. This paper is proposed to defeat the inadequacy by proposing a new algorithm so that efficiency is improved. Accurate foreground extraction is a challenging issue in all bias correction techniques and another problem is, these algorithms are eroding bias in iterative approaches and this makes

the algorithm computationally complex. This paper recommends an uncomplicated technique to conquer the drawback. The proposed algorithm is a factual Foreground Segregation and Gradient based Bias Correction point out as FSGBC throughout this section. FSGBC is analyzed with N3 algorithm.

The remaining paper is formulated as, section 2 includes theoretical background regarding bias model formulation, section 3 incorporates detailed study of our proposed algorithm, section 4 contains the result & discussion and section 5 summarizes the result.

2. BIAS FIELD MODEL

The fundamental reason of bias correction is reclaiming the original image intensities. The bias field can be formed as a smoothly varying multiplicative function. The bias corrupted image signals captured by scanner is modeled as,

$$F(x,y) = I(x,y)\, B(x,y) + N(x,y) \quad (1)$$

F(x,y) is bias corrupted image, I(x,y) is a true image, B(x,y) is a bias function, it is smoothly varying multiplicative field. N(x,y) is noise term which is zero mean additive or Gaussian noise. The noise term is mostly neglected in bias correction techniques. If bias field is known then the initial image signals can be easily restored.

$$I(x,y) = F(x,y) / B(x,y) \quad (2)$$

By applying logarithmic transformation on the equation (1), the model is transformed additive as follows,

$$F_{log}(x,y) = I_{log}(x,y) + B_{log}(x,y) \quad (3)$$

$F_{log}(x,y)$, $I_{log}(x,y)$, $B_{log}(x,y)$ are logarithmic transformation of F (x,y), I (x,y) and B (x,y).

3. FACTUAL FOREGROUND SEGREGATION AND GRADIENT BASED BIAS CORRECTION (FSGBC)

This proposed method concentrates on accurate foreground segregation and bias correction. The Figure.1 represents the flow of the proposed technique.

A. Input Image:

Bias corrupted 2D DICOM brain MR Images are given as an input.

B. Gradient Calculation:

Bias field is described as a smooth shading effect constructed over an original image. In shading effect the image intensities are darker in one side and gets lighter on another side. Gradient operation is adopted to assess the directional modulation of pixel intensities. And smoothing operation is performed to remove the present bias by Gaussian. These operations are performed over an entire image. The intensity variation can be evaluated in horizontal (x) and vertical (y) direction.

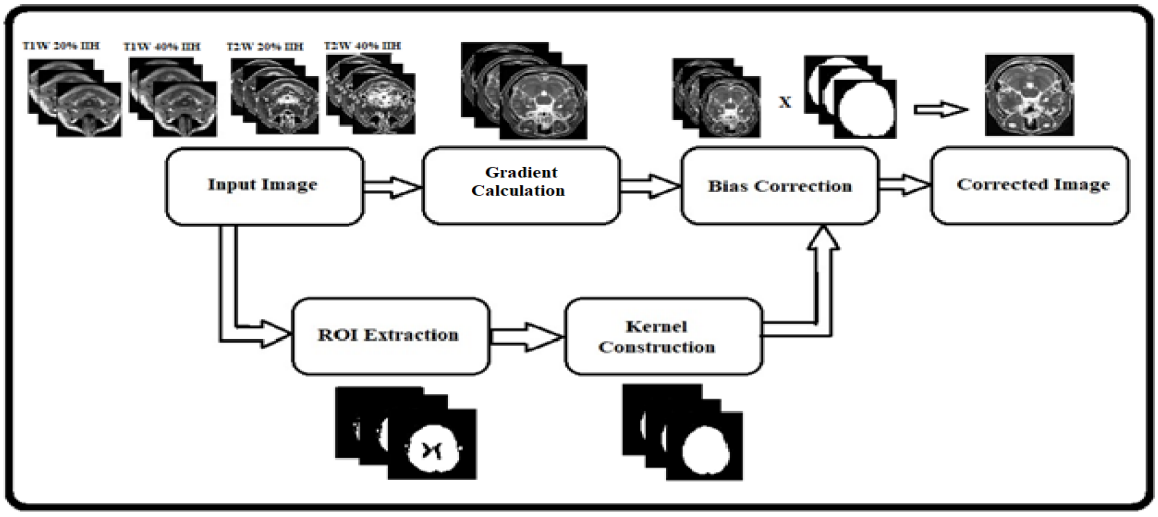

FIGURE 1: Work Flow of the FSGBC Algorithm

Gradient calculation in x direction

$$\nabla f = \frac{\partial f}{\partial x} \tag{4}$$

Gradient calculation in y direction

$$\nabla f = \frac{\partial f}{\partial y} \tag{5}$$

Gradient calculation in both x and y direction

$$\nabla f = \left[\frac{\partial f}{\partial x}, \frac{\partial f}{\partial y}\right] \tag{6}$$

$$\theta = tan^{-1}\left(\frac{\partial f}{\partial y} \,/\, \frac{\partial f}{\partial x}\right) \quad (7)$$

In this method gradient is calculated clock wise with [-180,180] degree in positive x direction.

C. ROI Extraction:

The Region Of Interest is an image component that is obtained from the initial image to accomplish certain operations. It is a binary kernel. By using the threshold value, foreground is extracted. The interested region intensity will be set to one and the remaining area intensity is assigned to zero. The input images are gray scale images. By considering this, the threshold values will be optimized.

D. Kernel Construction:

The bias field can change the image intensities. Boundary pixels are also deteriorated. The extracted Region Of Interest may not be precise because of the Intensity In Homogeneity present in image. Subsequent post processing operations should be performed to amend the Region Of Interest for kernel construction. The microscopic elements present near the extracted region should be removed using the morphological operation imopen. Assign labels for regions, using the region property area. The brain organ itself contains airvoxels. The intensity of the airvoxels is darker in MRI. These parts are excluded while extracting ROI. The missed regions within the ROI should be incorporated. Adding these regions is an essential operation to be carried out while constructing the kernel. Edge parameters are corrected using the morphological operation imclose. This helps to abolish the small suspensions present in edges.

E. Bias Correction:

The bias corrected image is recovered by augmenting gradient corrected image with constructed kernel. So that accurate foreground extracted and bias corrected images will be recovered.

4. Result and Discussion

Our proposed method is tested on bench mark dataset collected from Brain Web website [25]. T1 and T2 weighted brain MR Images with twenty and forty percent Intensity in Homogeneity each are used here. These images are with thickness one mille meter, and zero percent noise

images. Each category contains 181 slices of brain MR Images. First 165 images are used for evaluation because of sufficient image organs. To assess the performance of our proposed FSGBC algorithm, the state of the art GCV (Grey matter Coefficient of Variation) WCV (White matter Coefficient of Variation) and CJV (Coefficient of Joint Variation) will be used. The brain incorporates three main organs such as White Matter, Gray Matter and Cerebrospinal fluid.

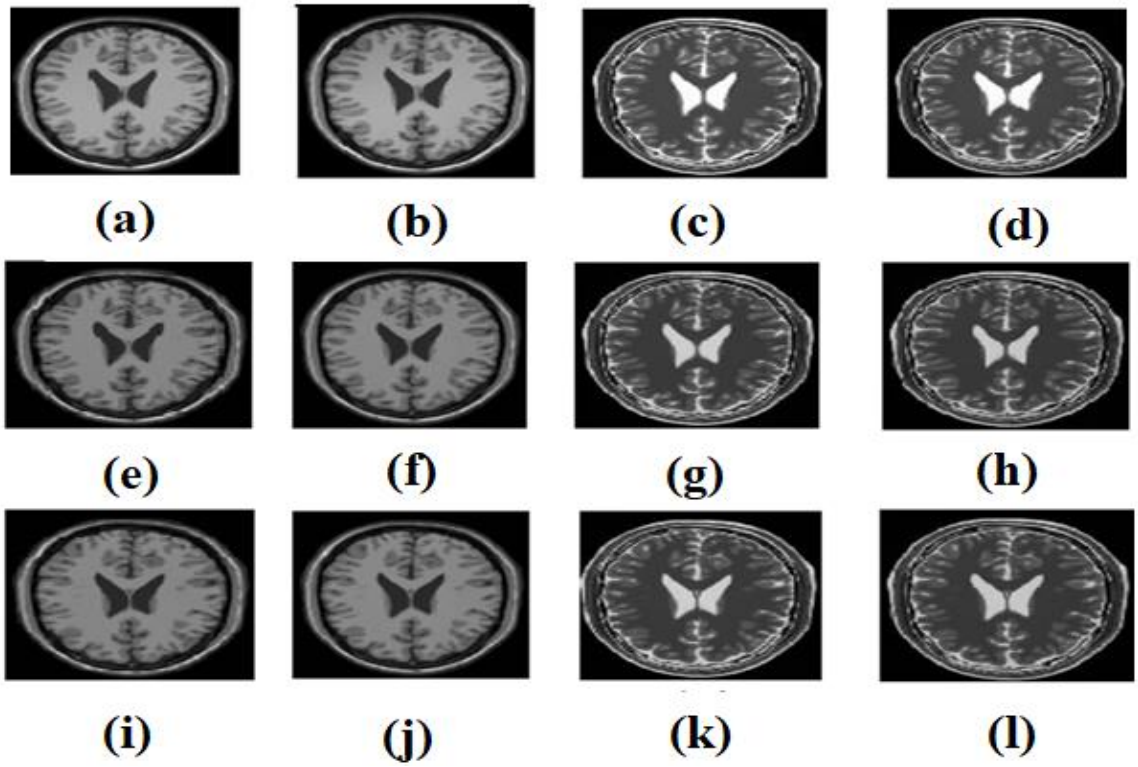

FIGURE 2: Input Image (a) – (d), (a) T1 Weighted images with 20% Intensity Non Uniformity, (b) T1 Weighted images with 40% Intensity Non Uniformity, (c) T2 Weighted images with 20% Intensity Non Uniformity, (d) T2 Weighted images with 40% Intensity Non Uniformity, (e) – (h) appropriate input images corrected with N3 bias correction algorithm , (i) –(l) appropriate input images corrected with FSGBC bias correction algorithm.

By measuring with white and gray matter, Cerebrospinal fluid is very microscopic area. Examining the cerebrospinal fluid for bias correction will not sufficiently provide authenticate

outcome. So CV and CJV will be calculated for white and gray matter alone. For each tissue or pixel x from White Matter (WM) or Grey Matter (GM), the Coefficient of Variation calculated by,

$$CV(x) = \frac{\sigma(x)}{\mu(x)} \tag{8}$$

The Coefficient of Joint Variation defined by,

$$CJV = \frac{\sigma(WM)+\sigma(GM)}{|\mu(WM)-\mu(GM)|} \tag{9}$$

Where $\mu(x)$ and $\sigma(x)$ are mean and standard deviation of tissue or pixel x. Our proposed technique will be scrutinized with the spotlight bias correction algorithm N3. All these dataset and software's are publicly available. The value of CV and CJV should be trivial to indicate the better performance.

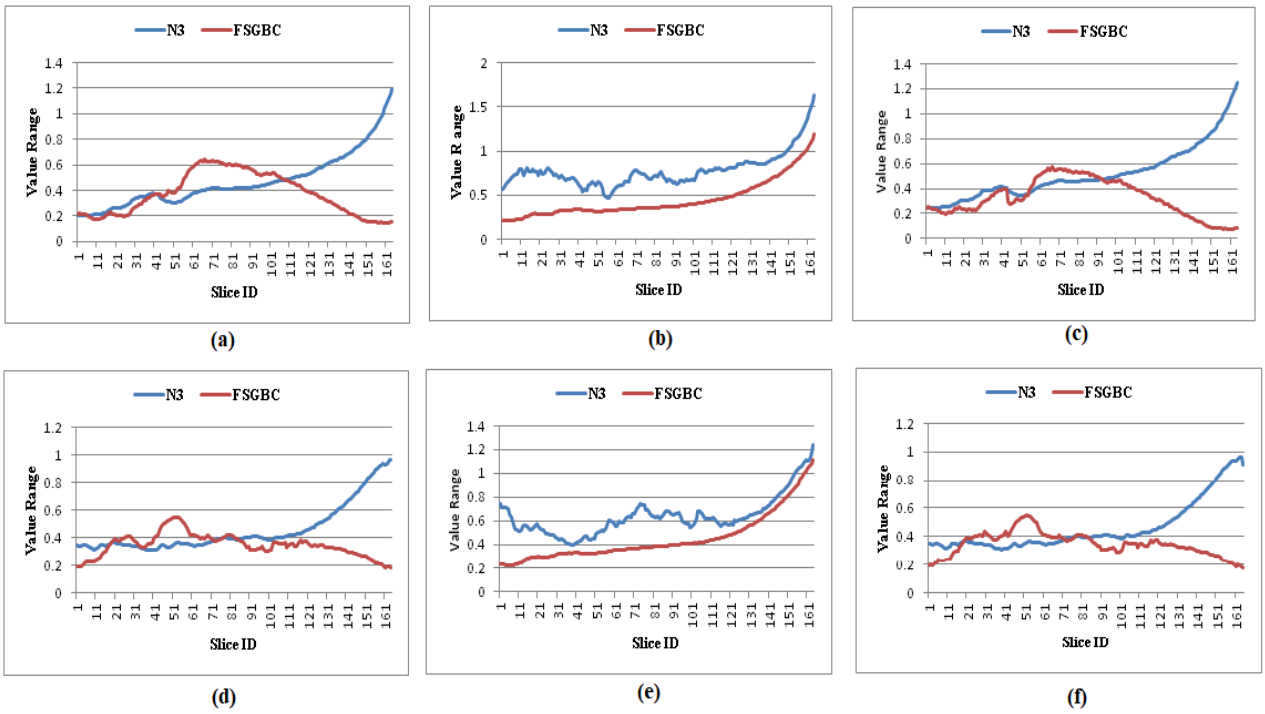

FIGURE 3: (a), (b), (c) – Slice wise GCV, WCV and CJV performance of N3, FSGBC algorithms over T1Weighted images with 20% Intensity Non Uniformity, (d), (e), (f) – Slice wise GCV, WCV and CJV performance of N3, FSGBC algorithms over T2 Weighted images with 20% Intensity Non Uniformity.

TABLE 1: N3 and FSGBC algorithms efficiency over T1 Weighted images with 20% Intensity Non Uniformity

	N3	**FSGBC**
GCV	0.4746	**0.3725**
WCV	0.7852	**0.4523**
CJV	0.4786	**0.3695**

TABLE 2: N3 and FSGBC algorithms efficiency over T1 Weighted images with 40% Intensity Non Uniformity

	N3	**FSGBC**
GCV	0.4800	**0.3650**
WCV	0.7966	**0.4516**
CJV	0.4840	**0.3619**

TABLE 3: N3 and FSGBC algorithms efficiency over T2 Weighted images with 20% Intensity Non Uniformity

	N3	**FSGBC**
GCV	0.4576	**0.3666**
WCV	0.6384	**0.4480**
CJV	0.4609	**0.3621**

TABLE 4: N3 and FSGBC algorithms efficiency over T2 Weighted images with 40% Intensity Non Uniformity

	N3	**FSGBC**
GCV	0.4583	**0.3469**
WCV	0.6403	**0.4525**
CJV	0.4617	**0.3439**

Figure 2 (a) - (d) lists the type of input images, (e) - (h) and (i) - (l) are appropriate input images corrected with N3 and FSGBC algorithm, when images are deteriorated by less than forty percent of bias, then it is barely visible to the spectator. So quantitative metrics are used in performance measurement. Figure 3 (a),(b),(c) lists the slice wise performance of CV for grey matter, CV for White matter and CJV for Bias correction algorithms N3 and FSGBC over the T1 Weighted input images of twenty percent Intensity Non Uniformity. Figure 3 (d),(e),(f) lists the slice wise performance of CV for grey matter, CV for White matter and CJV for Bias correction algorithms N3 and FSGBC over the T2 Weighted input images of twenty percent Intensity Non Uniformity. Fig 3(b) and (e) clearly confesses that FSGBC algorithm performed well because its WCV value range is lesser compared with N3 algorithm. But in the case of other metrics GCV and CJV, the FSGBC and N3 algorithms efficiency is keep on diverging. For specific slices the N3 algorithm performed well, and for remaining slices FSGBC performed well. The algorithms performances are same for T2 Weighted images also. This result might be by the lack of consistency of grey matter and white matter in the input images. Based on slice wise performance the outcome cannot be concluded. So overall performance of each input type is calculated.

Table 1, 2, 3 and 4 lists the gross efficiency of N3 and FSGBC algorithm over four types of input images. Table 1 clearly states that FSGBC algorithms efficiency is higher while comparing with N3 algorithm, because it’s grey CV, white CV and CJV value is lesser than N3 algorithm. Table 2, 3 and 4 admits a similar result that, for different sorts of input images also FSGBC algorithm provides better performance. Fig 4 shows the comprehensive performance on N3 and FSGBC algorithm over the T1 & T2 Weighted input images with twenty and forty percent Intensity Non Uniformity. It portraits the performance of CV for grey matter, white matter and CJV of bias correction algorithms N3 and FSGBC. The outcome clearly states that FSGBC algorithms efficiency is higher while comparing with N3 algorithm. FSGBC’s GCV (±0.3628), WCV (±0.4511) and CJV (±0.3594) is lesser than N3 algorithms GCV (±0.4677), WCV (±0.7152) and CJV (±0.4713).

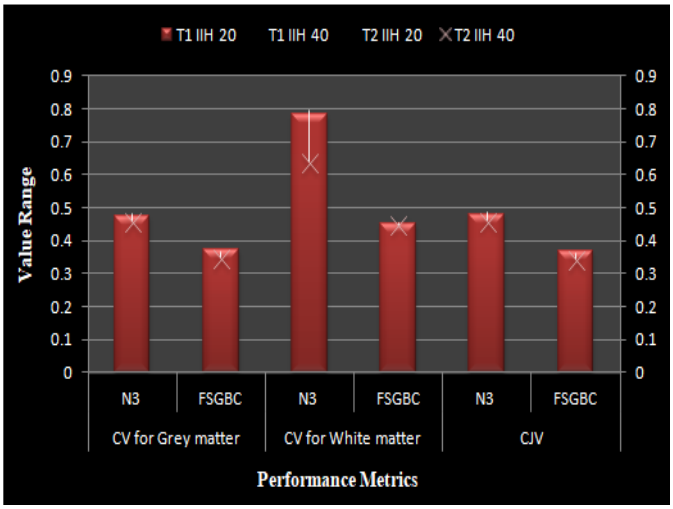

FIGURE 4: Overall performance of N3 and FSGBC algorithm

Let *g (x, y)* represents the ground truth of the brain MRI, and *b (x, y)* represents the twenty percent bias corrupted brain MR Image.

$$g(x,y) \sim b(x,y) = t(x,y) \quad (10)$$

$$b(x,y) \sim n(x,y) = c1(x,y) \quad (11)$$

$$b(x,y) \sim f(x,y) = c2(x,y) \quad (12)$$

$$t(x,y) \sim c1(x,y) = u1(x,y) \quad (13)$$

$$t(x,y) \sim c2(x,y) = u2(x,y) \quad (14)$$

Differentiating ground truth and twenty percent bias corrupted image segregate the added twenty percent bias (*t (x, y)*) alone. *n (x, y)* represents the bias corrected image using N3 algorithm. *f (x, y)* represents the bias corrected image using FSGBC algorithm. $c1(x,y)$ and $c2(x,y)$ represents the bias region corrected by N3 and FSGBC algorithm. Differentiating this with added twenty percent bias yields the region which is not corrected by N3 $(u1(x,y))$ and FSGBC algorithm $(u2(x,y))$. Qualitative measurement of the FSGBC algorithm and N3 algorithm is discussed in Figure 5. Figure 5(a) represents the bias region uncorrected by N3 algorithm; Figure 5(b) represents bias region uncorrected by FSGBC algorithm. These images clearly distinguish that, FSGBC algorithms' uncorrected region is lesser than the reputed N3 algorithm. For clear investigation, the uncorrected region is represented in binary image format.

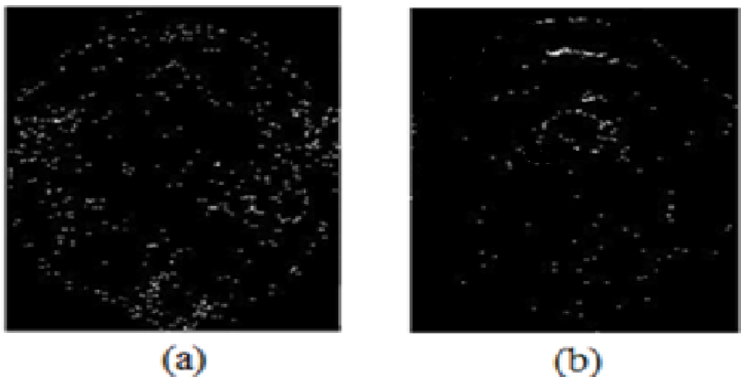

FIGURE 5: (a) Uncorrected bias area by N3 algorithm,

(b) Uncorrected bias area by FSGBC algorithm**.**

5. CONCLUSION

This paper nominates a novel technique which automatically segregate foreground from the bias corrupted image and eradicate the bias presents in that image. The algorithm performs this task at several stages: gradient calculation, ROI extraction, kernel construction and bias correction. ROI extraction and Kernel construction used for accurate foreground segregation which incorporates multiple operations to concentrate on microscopic elements, air voxels and discontinuities available in and around of extracted ROI. Gradient calculation helps to remove the bias from the image. Bias corrected image is amended by augmenting gradient corrected image with kernel. No manual intervention is required throughout the procedure. The proposed technique will be scrutinized with N3 algorithm. The proposed algorithms efficiency is measured in quantitative and qualitative manner. The performance metrics CV and CJV is used to assess the algorithms efficiency in quantitative manner. CV is distinctively calculated for two brain tissues white and grey matter, while the CJV is measured over incorporating white and grey matter. Lesser CV and CJV shows off the best performance. The result concludes that FSGBC algorithm outperforms the N3 algorithm because it's WCV, GCV and CJV value is lesser. The FSGBC algorithm proves its efficiency in qualitative aspect also. From the quantitative and qualitative measurement, the result concluded that the FSGBC algorithm amend the hurdle present and outperforms the N3 algorithm in bias correction. This paper concentrated mostly over bias

estimation only, for bias correction it uses fundamental gradient strategy. The future scope of this paper is to apply bi cubic spline, polynomial estimation and surface fitting strategies in bias correction which helps to completely wipe out the shading effect and elevate the algorithms efficiency to the greater level.

FUNDING

Not applicable

CONFLICT OF INTERESTS

The author(s) declare that there is no conflict of interests.

REFERENCES

[1] G.H. Glover, C.E. Hayes, N.J. Pelc, et al. Comparison of linear and circular polarization for magnetic resonance imaging, J. Magn. Reason. (1969). 64 (1985), 255–270.

[2] I. Harvey, P.S. Tofts, J.K. Morris, D.A.G. Wicks, M.A. Ron, Sources of T1 variance in normal human white matter, Magn. Reason. Imaging. 9 (1991), 53–59.

[3] A. Simmons, P.S. Tofts, G.J. Barker, S.R. Arridge, Sources of intensity nonuniformity in spin echo images at 1.5 T, Magn. Reson. Med. 32 (1994), 121–128.

[4] G.J. Barker, A. Simmons, S.R. Arridge, P.S. Tofts, A simple method for investigating the effects of non-uniformity of radiofrequency transmission and radiofrequency reception in MRI, Br. J. Radiol. (BJR). 71 (1998), 59–67.

[5] M. Alecci, C.M. Collins, M.B. Smith, P. Jezzard, Radio frequency magnetic field mapping of a 3 Tesla birdcage coil: Experimental and theoretical dependence on sample properties, Magn. Reson. Med. 46 (2001), 379–385.

[6] M. Ganzetti, N. Wenderoth, D. Mantini, Quantitative Evaluation of Intensity Inhomogeneity Correction Methods for Structural MR Brain Images, Neuroinform. 14 (2016), 5–21.

[7] Z.P. Liang, P.C. Lauterbur, Principles of magnetic resonance imaging: a signal processing perspective. IEEE Press, New York, 2000.

[8] E.R. McVeigh, M.J. Bronskill, R.M. Henkelman, Phase and sensitivity of receiver coils in magnetic resonance imaging: Phase and sensitivity of receiver coils in MRI, Med. Phys. 13 (1986), 806–814.

[9] L. Axel, J. Costantini, J. Listerud, Intensity correction in surface-coil MR imaging, Amer. J. Roentgenol. 148 (1987), 418–420.

[10] D.A.G. Wicks, G.J. Barker, P.S. Tofts, Correction of intensity nonuniformity in MR images of any orientation, Magn. Reason. Imaging. 11 (1993), 183–196.

[11] Z. Hou, A Review on MR Image Intensity Inhomogeneity Correction, Int. J. Biomed. Imaging. 2006 (2006), 49515.

[12] U. Vovk, F. Pernus, B. Likar, A Review of Methods for Correction of Intensity Inhomogeneity in MRI, IEEE Trans. Med. Imaging. 26 (2007), 405–421.

[13] H. Liu, S. Liu, D. Guo, Y. Zheng, P. Tang, G. Dan, Original intensity preserved inhomogeneity correction and segmentation for liver magnetic resonance imaging, Biomed. Signal Proc. Control. 47 (2019) 231–239.

[14] L. Wang, J. Zhu, M. Sheng, A. Cribb, S. Zhu, J. Pu, Simultaneous segmentation and bias field estimation using local fitted images, Pattern Recognit. 74 (2018), 145–155.

[15] C. Li, C. Xu, A.W. Anderson, J.C. Gore, MRI Tissue Classification and Bias Field Estimation Based on Coherent Local Intensity Clustering: A Unified Energy Minimization Framework, in: J.L. Prince, D.L. Pham, K.J. Myers (Eds.), Information Processing in Medical Imaging, Springer Berlin Heidelberg, Berlin, Heidelberg, 2009: pp. 288–299.

[16] Z.-X. Ji, Q.-S. Sun, D.-S. Xia, A modified possibilistic fuzzy c-means clustering algorithm for bias field estimation and segmentation of brain MR image, Comput. Med. Imaging Graph. 35 (2011), 383–397.

[17] C. Huang, L. Zeng, An Active Contour Model for the Segmentation of Images with Intensity Inhomogeneities and Bias Field Estimation, PLoS ONE. 10 (2015), e0120399.

[18] C. Li, R. Huang, Z. Ding, J.C. Gatenby, D.N. Metaxas, J.C. Gore, A Level Set Method for Image Segmentation in the Presence of Intensity Inhomogeneities With Application to MRI, IEEE Trans. Image Process. 20 (2011), 2007–2016.

[19] J.G. Sled, A.P. Zijdenbos, A.C. Evans, A nonparametric method for automatic correction of intensity nonuniformity in MRI data, IEEE Trans. Med. Imaging. 17 (1998), 87–97.

[20] N.J. Tustison, B.B. Avants, P.A. Cook, et al. N4ITK: Improved N3 Bias Correction, IEEE Trans. Med. Imaging. 29 (2010), 1310–1320.

[21] Farzana, M. Sathik, S. Nisha, Performance analysis of bias correction techniques in brain MR images, Int. J. Inform. Technol. 12 (2020), 899–905.

[22] O. Salvado, C. Hillenbrand, S. Zhang, D.L. Wilson, Method to correct intensity inhomogeneity in MR images for atherosclerosis characterization, IEEE Trans. Med. Imaging. 25 (2006), 539–552.

[23] C. Li, J.C. Gore, C. Davatzikos, Multiplicative intrinsic component optimization (MICO) for MRI bias field estimation and tissue segmentation, Magn. Reason. Imaging. 32 (2014), 913–923.

[24] M.N. Ahmed, S.M. Yamany, N. Mohamed, A.A. Farag, T. Moriarty, A modified fuzzy c-means algorithm for bias field estimation and segmentation of MRI data, IEEE Trans. Med. Imaging. 21 (2002), 193–199.

[25] C.A. Cocosco, V. Kollokian, R.K.-S. Kwan, A.C. Evans, BrainWeb: Online interface to a 3D MRI simulated brain database. NeuroImage, 5 (1997), S425.